ACS APPLIED MATERIALS & INTERFACES

RESEARCH ARTICLE

www.acsami.org

Efficient Photochromic Transformation of a New Fluorenyl Diarylethene: One- and Two-Photon Absorption Spectroscopy

Gheorghe Luchita,[†] Mykhailo V. Bondar,[‡] Sheng Yao,[†] Ivan A. Mikhailov,[§] Ciceron O. Yanez,[†] Olga V. Przhonska,[‡] Artem E. Masunov,[†,§,⊥,#] and Kevin D. Belfield*[,†,||]

[†]Department of Chemistry, [||]CREOL, The College of Optics and Photonics, [§]NanoScience Technology Center, [⊥]Department of Physics, and [#]Florida Solar Energy Center, University of Central Florida, P.O. Box 162366, Orlando, Florida 32816, United States

[‡]Institute of Physics, Prospect Nauki, 46, Kiev-28, 03028, Ukraine

ABSTRACT: Efficient reversible phototransformation of a new diarylethene-fluorene derivative, 1,2-bis(5-(9,9-didecyl-7-nitro-9H-fluoren-2-yl)-2-methylthiophen-3-yl)cyclopent-1-ene (**1**), was demonstrated in organic media under low-intensity laser excitation. Linear photophysical characterization of **1** was performed at room temperature in solvents of different polarity and viscosity. Significantly, close to unity quantum yield for the cyclization reaction of **1** was shown in nonpolar solutions. The lifetimes of the excited states of the open (OF) and closed (CF) forms of **1** were measured by a femtosecond transient absorption technique, and corresponding values of ~0.7 and ~0.9 ps were shown in dichloromethane (DCM), respectively. Degenerate two-photon absorption (2PA) spectra of the OF and CF of **1** were obtained over a broad spectral range by the open aperture Z-scan method under 1 kHz femtosecond excitation. The values of 2PA cross sections of the OF in DCM (~50−70 GM) were found to increase up to 1 order of magnitude (~600 GM) after cyclization to the CF. The nature of cyclization and cylcoreversion processes were investigated by quantum chemistry with employment of DFT-based methods implemented in the Gaussian'09 program. The potential of **1** for application in optical data storage was shown using poly(methyl methacrylate)-doped films and two-photon fluorescence microscopy readout.

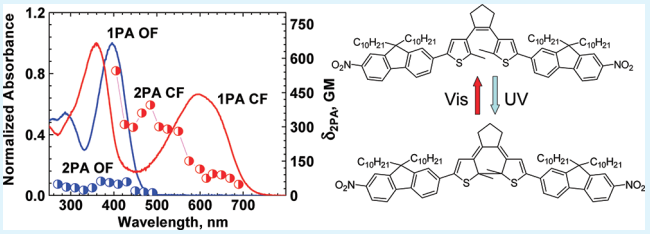

KEYWORDS: photochromic reaction, photoisomerization, diarylethene, two-photon absorption, transient absorption spectroscopy

1. INTRODUCTION

The processes of one- and two-photon photochromic transformations in organic molecules are currently a subject of great interest for various applications, such as the development of switching devices in optoelectronics,[1−5] optical signal processing,[6,7] and high-density 3D optical data storage.[8−11] Organic molecules that can be used for such applications are expected to have a large absorption cross section and high quantum yield of the photochromic transformation. The development of two-photon absorbing photochromes has been one of the most interesting and challenging tasks, combining molecular phototransformation mechanisms with the advantages of two-photon absorption (2PA) processes.[12−14] Examples of the design of a new photochromic molecule having a high 2PA efficiency employed linking porphyrin and photochromic perinaphthothioindigo moieties via an acetylenic bond[15] and the two-photon-induced photoisomerization of 3-[1-(1,2-dimethyl-1H-indol-3-yl)-ethylidene]-4-isopropylidene-dihydrofuran-2,5-dione.[16] Among the wide variety of photochromic compounds (azobenzenes,[17] spiropyrans,[2] fulgides,[18] and others), diarylethene derivatives are a promising class of thermally irreversible photochromic molecules developed by Irie et al.[19,20] and Lehn et al.[21,22] for potential use in high-density optical memory devices. These compounds are characterized by efficient photoisomerization and excellent thermal stability, write-erase fatigue resistance, high sensitivity, fast response, and non-destructive readout capability.[23−26]

However, little has been reported on diarylethene derivatives with large values of 2PA cross sections and high quantum yield of the photochromic transformation. For example, diarylethene dimer derivatives with 1,4-bis-(ethynyl)benzene or 1,4-bis(ethenyl) benzene as a π-conjugated chain units were described.[27] These compounds exhibited efficient phototransformation (with corresponding quantum yields of ~0.3−0.7) but relatively small values of 2PA cross-sections (~ 23−44 GM). The main difficulties in the development of photochromic 2PA diarylethenes involve the high sensitivity of cyclization and cycloreversion quantum yields on the molecular geometry of diarylethene core,[28,29] which typically changes even upon subtle structural modifications of the photochromic molecule.[30,31] Therefore, introduction of an extended π-electron system, with large 2PA, in the diarylethene-based structure often leads to a dramatic decrease in the photoisomerization quantum yield. Herein, we present the synthesis along with the linear photophysical and nonlinear optical characterization of a new diarylethene-fluorenyl derivative, 1,2-bis(5-(9,9-didecyl-7-nitro-9H-fluoren-2-yl)-2-methylthiophen-3-yl)cyclopent-1-ene (**1**), that

Received: June 17, 2011
Accepted: August 10, 2011
Published: August 10, 2011

Scheme 1. Synthesis of Diarylethene 1

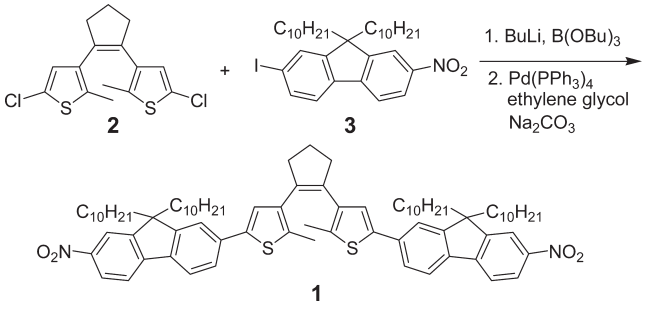

exhibited high efficiency of the photochromic transformation and relatively large 2PA cross sections, δ_{2PA}. Cyclization and cycloreversion processes were investigated by means of steady-state linear absorption spectroscopy, quantum-chemical calculations based on DFT, and femtosecond transient absorption pump−probe methods successfully developed over the past few years by Irie et al.[32−34] for experimental studies of photochromic materials. Degenerate 2PA spectra of the open (OF) and closed (CF) form of **1** were obtained over a broad spectral range by an open aperture Z-scan method under femtosecond excitation. A large increase in 2PA efficiency (up to 1 order of magnitude) for the closed form isomer of **1** was shown. Cursory examination of the new photochromic diarylethene for optical data storage was demonstrated under femtosecond two-photon excitation using a poly(methyl methacrylate) composite containing a mixture of **1** and Rhodamine 6G.

2. EXPERIMENTAL SECTION

2.1. Synthesis of 1. The synthesis of the photochromic diarylethene **1** is shown in Scheme 1. 1,2-Bis(5-chloro-2-methylthiophen-3-yl)cyclopent-1-ene (**2**) was converted to boronic acid *in situ* and directly coupled with 9,9-didecyl-2-iodo-7-nitro-9H-fluorene (**3**) using $Pd(PPh_3)_4$ and ethylene glycol as catalysts in a one-pot reaction to give the product **1** with a yield of 77%, as described below. The structure was confirmed by ^1H, ^{13}C NMR, and high-resolution MS. Intermediates **2** and **3** were prepared according to literature methods.[35,36]

Synthesis of Diarylethene ***1***. 1,2-Bis(5-chloro-2-methylthiophen-3-yl)cyclopent-1-ene **2** (0.66 g, 2.0 mmol) in dry THF was added to n-BuLi (1.6 M in hexane, 2.5 mL, 4.0 mmol) at −78 °C under Ar and stirred for 30 min. The mixture was then stirred at room temperature for 20 min before addition of $B(OBu)_3$ (1.73 mL, 6.4 mmol), and the reaction was continued at room temperature for one more hour. Meanwhile 9, 9-didecyl-2-iodo-7-nitro-9H-fluorene **3** (2.78 g, 4.5 mmol) in THF and ethylene glycol (10 drops) mixed with 2 M Na_2CO_3 aqueous solution (10 mL) was purged with Ar for 30 min. The above-mentioned two solutions and $Pd(PPh_3)_4$ (0.126 g, 0.11 mmol) were mixed under Ar and heated at reflux for 16 h. Water was added, and the product was extracted with hexane, washed with water, and dried over $MgSO_4$. The crude product was purified by column chromatography using hexanes/CH_2Cl_2 (from 6/1 to 3/1) to afford 1.92 g of product **1** as yellow sticky oil (77% yield). ^1H NMR (300 MHz, $CDCl_3$) δ 8.18 (m, 2H), 8.11 (s, 2H), 7.66 (m, 4H), 7.49 (m, 2H), 7.41 (s, 2H), 7.11 (s, 2H), 2.84 (t, J = 7.5 Hz, 4H), 2.06 (m, 2H), 2.01 (s, 6H), 1.94 (t, J = 9.0 Hz, 8H), 1.18−0.97 (m, 56H), 0.76 (t, J = 6.0 Hz, 12H), 0.54 (m, 8H). ^{13}C NMR (75 MHz, $CDCl_3$) δ 153.4, 152.2, 147.4, 147.2, 139.9, 137.9, 137.2, 135.7, 135.5, 134.9, 125.0, 124.9, 123.6, 121.8, 119.8, 118.4, 105.0, 56.0, 40.3, 38.8, 32.1, 30.1, 29.7, 29.5, 29.4 24.0, 22.9, 14.9, 14.3. HRMS (ESI) for $C_{81}H_{110}N_2O_4S_2$ theoretical m/z $[M + Na]^+$=1261.7799, found $[M + Na]^+$ = 1261.7790.

2.2. Linear Photophysical Measurements. All photophysical parameters of **1** were obtained in spectroscopic grade hexane, cyclohexane, and dichloromethane (DCM) at room temperature. The steady-state absorption spectra of **1** were measured with an Agilent 8453 UV−visible spectrophotometer in 1 and 10 mm path length quartz cuvettes with dye concentrations 2×10^{-5} M ≤ C ≤ 2.5×10^{-4} M. The steady-state fluorescence and excitation spectra were obtained with a PTI QuantaMaster spectrofluorimeter in 10 mm spectrofluorometric quartz cuvettes with $C \approx 1-2 \times 10^{-6}$ M. All fluorescence spectra were corrected for the spectral responsivity of the PTI detection system (emission monochromator and PMT). The values of fluorescence quantum yields of **1** were measured in dilute solutions by a standard method relative to 9,10 diphenylanthracene in cyclohexane.[37] Cyclization and cycloreversion reaction quantum yields of **1** were obtained by known experimental methodology[38] under cw 405 and 532 nm low-intensity laser irradiation, respectively.

2.3. Transient Absorption Measurements. Investigations of dynamic processes in photochrome **1** were performed on the basis of pump−probe transient absorption methodology[39,40] using the femtosecond laser system depicted in Figure 1a. The output of a mode-locked Ti:sapphire laser (Mira 900-F, Coherent, wavelength 800 nm, average power ≈ 1.1 W, pulse duration 200 fs, repetition rate 76 MHz) pumped by the SHG of cw Nd^{3+}:YAG laser (Verdi-10, Coherent) was regeneratively amplified with 1 kHz repetition rate (Legent Elite USP, Coherent) providing ≈100 fs pulses (fwhm) with an energy of ∼2.8 mJ/pulse. This output was split into two separate laser beams with ∼1.8 W and ∼0.8 W average powers, respectively. The first beam pumped an ultrafast optical parametric amplifier (OPerA Solo, Coherent) with a tuning range 240 nm to 20 μm, pulse duration $\tau \approx$ 100 fs (fwhm) and pulse energies, E, up to ∼40 μJ. The second laser beam (800 nm) was converted via SHG for use as a 400 nm pump source. The time profile of the transient absorbance of the OF of **1** excited at 400 nm (2.5 μJ, pump pulse) was obtained by monitoring at 425 nm (<2 nJ, probe pulse). The polarization of the two pulses was linear and oriented at the magic angle relative to each other for all measurements. The pump and probe beams were focused to waists of radii ∼0.7 mm and 0.2 mm (fwhm), respectively, and recombined at a small angle (<5−7°) within the sample solutions in a 1 mm path length quartz cell. The transient absorbance profile of the CF of **1** was measured with the pump (≈ 2.5 μJ) and probe (<2 nJ) pulses at the same wavelength (600 nm) from the OPA output split in two beams. A possible coherent pump−probe interaction[41] inside the cuvette was negligible under the experimental conditions employed. The absorbance of the samples at the excitation wavelengths was set to be ∼0.8−1.0 and the sample solution was circulated through a 1 mm quartz cell at a flow rate of ∼200 mL/min. The duration of the cross-correlation between pump and probe pulses, τ_{cc}, was measured with a pump−probe technique based on the optical Kerr effect[42,43] in a 1 mm optical path length quartz cell filled with CCl_4 and corresponded to ≈100 fs (fwhm) Gaussian pulses. A typical example of the cross-correlation trace monitored at the sample position is shown in Figure 1b.

2.4. 2PA Measurements. The degenerate 2PA spectra of the OF and CF of **1** were obtained by an open aperture Z-scan method[44] under 1 kHz femtosecond excitation (see Figure 1a, right side) with fitting experimental values of transmittance, $T(z)$, according to the known equation:[45]

$$T(z) = \frac{1}{\sqrt{\pi}\beta I_0(z) L}\int_{-\infty}^{+\infty} \ln[1 + \beta I_0(z) L \exp(-t^2)]dt$$

where β is the 2PA coefficient; L is the length of the sample and, z and t are, the longitudinal space coordinate and time, respectively. $I_0(z) = (2E)/(\pi^{3/2}\omega(z)^2\tau)$, where $\omega(z)$ is the transverse size of the beam (HW1/e^2 M). 2PA cross sections were determined as: $\delta_{2PA} = \beta \cdot h\nu/(C)$ ($h\nu$ is the photon energy and C is the molecular concentration in the sample). The output of the OPA tuned over the range 540−1400 nm, pulse duration ∼100 fs

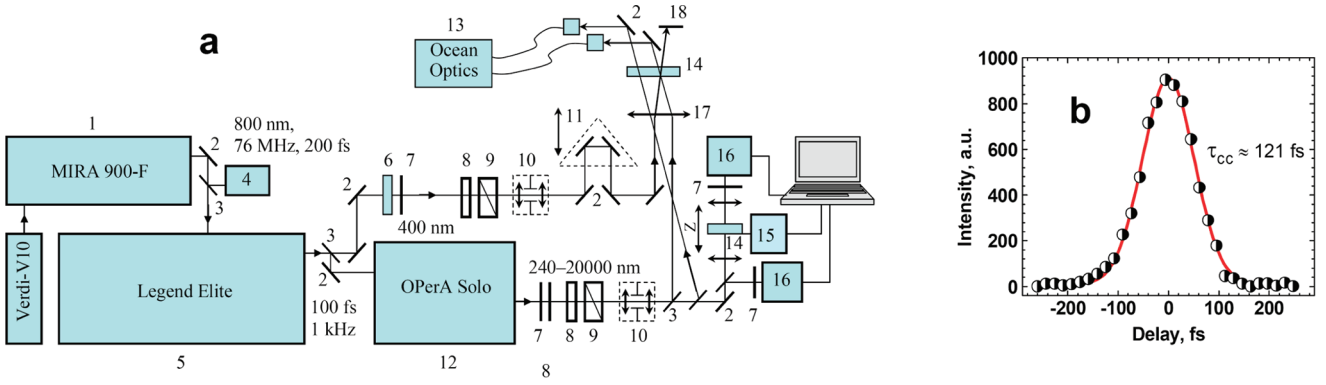

Figure 1. (a) Schematic diagram of the experimental setup: 1, femtosecond 76 MHz laser; 2, 100% reflection mirrors; 3, beam splitters; 4, spectrometer; 5, regenerative amplifier; 6, BBO crystal; 7, set of neutral and/or interferometric filters; 8, wave plates $\lambda/2$; 9, polarizers; 10, space filters; 11, optical delay line with retro-reflector; 12, optical parametric amplifier; 13, fiber optic dual-channel spectrometer SD2000 (Ocean Optics, Inc.); 14, 1 mm quartz cuvettes with investigated solutions; 15, step motor; 16, calibrated Si and/or InGaAs photodetectors; 17, focusing lenses; 18, beam dump. (b) Cross-correlation trace for pump−probe pulses at 600 nm. The solid curve is a fit to Gaussian pump−probe pulses with $\tau \approx 100$ fs (fwhm).

(fwhm), and pulse energies ≤100 nJ was used. Solutions were placed in a 1 mm path length flow cell at ~1×10^{-2} M concentrations of **1**.

2.5. Optical Data Recording. Photosensitive polymer films, consisting of **1** (5.3×10^{-3} M) and Rhodamine 6G (1.0×10^{-3} M) in PMMA (average molecular weight =5,000 g/mol), were solution-casted (from CH_2Cl_2) onto 2.5 × 2.5 cm microscope glass coverslips. Two-photon recording and readout were performed on a modified Olympus Fluoview FV300 laser scanning confocal microscopy system equipped with a broad-band, tunable Coherent Mira Ti:sapphire laser (recording and readout at 750 nm; ≈ 130 mW, 200 fs pulse width, 76 MHz repetition rate), pumped by a 10 W Coherent Verdi frequency-doubled Nd:YAG laser. The FV300 was coupled to an Olympus IX-70 microscope (40x objective). In two-photon writing, the 2 ms exposure time and position were controlled by means of an electronic shutter and electronic stage, respectively, both from Thor Laboratories, that was in turn controlled by means a customized program. Two-photon optical recording was achieved by inducing conversion OF to CF with a corresponding decrease in the fluorescence intensity of Rhodamine 6G. Though Forster resonance energy transfer is possible with the concentrations used, the effect is likely simple reabsorption of the fluorescence emission of Rhodamine 6G by the CF of **1**. Readout was performed by inducing the upconverted fluorescence of Rhodamine 6G. The image was imported to SlideBook 4.2, where a Gaussian filter was employed in order to reduce noise. This was followed by a channel inversion after which the "fluorescent" pixels were inverted in intensity to resemble background and the "non-fluorescent" pixels were shown as having the highest intensity.

3. DETAILS OF QUANTUM-CHEMICAL CALCULATIONS

To evaluate the probability of photochromic transformation, one has to study the dynamics of excited states. To this end a computational method producing reliable potential energy surfaces with a sufficient accuracy is needed. Among existing computational approaches there are ab initio (e.g., RASSCF, DDCI), DFT-based (TD-DFT, MRDFT, etc.), semiempirical (TD-DFTB, OM2/MRCI), empirical (e.g., MMVB), and hybrid (e.g., ONIOM, QM/MM, or QM/QM) methods.[46,47] Here, we restricted our investigation by calculation of a minimum energy pathway (MEP) of the lowest excited state along a reaction coordinate. MEP provides qualitative information on the rates of photoinduced cyclization and cycloreversion. We use an approach developed and tested in ref 48, which includes structure optimization of the lowest excited state by the Slater transition state (STS) followed by TD-DFT correction to the excitation energy. The STS is a method of fractional occupation numbers approximating electronically excited states. We used DFT spin−orbitals in STS scheme, so that one α and one β electrons reside in the HOMO and LUMO with equal probabilities. One can conclude from the results published in ref 48 that although the STS-DFT method predicts reasonable excited-state geometry, it does not reproduce the total energy of the excited state accurately enough, and TD-DFT correction is required. It is worth noting that the chosen STS method provides good stabilization at the region of the pericyclic minimum (close to the transition state on the ground-state surfaces). This is related to the double excited nature of the first excited state in the region close to the ground-/excited-state intersection, which is represented by the STS scheme.

We began our DFT calculations by choosing a functional. The authors of ref 49 recommended TD-M05/6-31G*/PCM//M05−2X/6-31G* where solvent is represented by the polarizable continuum model (PCM) for prediction of the structural and spectral parameters for both OF and CF of diarylethene derivatives. We carried out geometry optimization at the M05−2X/6-31G*/PCM level. Structures of the OF and CF isomers of **1** optimized in n-hexane are shown in Figure 2. A fine-tuning of the Hartree−Fock (HF) fraction in the M05 functional was shown in ref 50 to allow a TD-DFT simulated absorption matching the experimental spectrum for a fluorene derivative. If the HF fraction in the M05 functional is termed X, then 2X is a fraction contained in the M05-2X. The value 1.25X was found necessary for the TD-DFT excitation energy to match the first experimental maximum. Similarly, in this contribution, we calculated the vertical excitations with TD-DFT, using functional M05-1.25X/PCM in the M05-2X/PCM optimized geometry. Our predictions reproduce precisely the wavelength of the first experimental maximum, corresponding to the linear absorption spectra for the OF isomer in hexane (381 nm) and DCM (396 nm). Although for the CF isomer the calculated excitation maximum is somewhat (15−20 nm) red-shifted with respect to the experiment, we used the M05−1.25X functional and *n*-hexane in PCM for all further calculations to predict the cyclization ability of the system.

All the calculations reported in the article were done with the Gaussian'09 program.[51] The standard 6-31G* basis set was

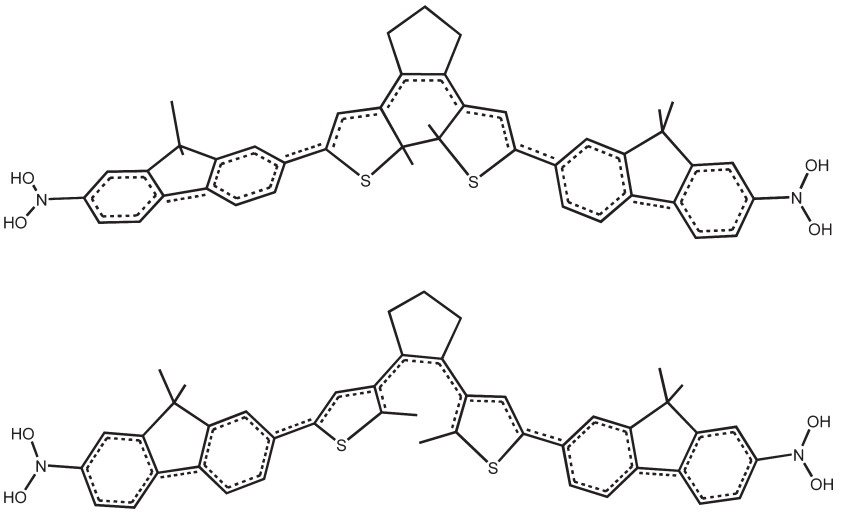

Figure 2. Optimized geometries of the CF and OF of **1**. The theory level is M05−2X/6-31G*/PCM (n-hexane). The cyclization bond length is 1.533 Å in the CF and 3.44 Å in the OF.

employed. The PCM with n-hexane solvent parameters was used to simulate the environment. Functional M05-1.25X was composed by calling M05 with IOp(3/76 = 0650003500) options. STS was set with IOp(5/75 = 1, 5/76 = 2, 5/77 = 1, 5/78 = 2). We started construction of the MEPs from the optimization of the OF and CF in their ground state (S_0). Then, starting from the structures obtained, we made the relaxed scan along the STS in two directions: from OF to CF and the reverse. The two energy profiles corresponding to both scanning directions coincided with each other, assuring us that we found the lowest-energy STS MEP. As was stated in ref 48 one has to use the spin-unrestricted approach for a proper description of the region, where the cyclization C−C bond is forming/breaking. Thus, we started each step of the scan by ensuring the stability of the Kohn−Sham orbitals with respect to α/β symmetry breaking, using "Stable=Opt" keyword. The resulting stable orbitals were then employed to construct the STS. To prevent a new (Huckel) orbital guess during the structure optimization, we used the Guassian keyword "Guess=NoExtra". For each optimized structure of the scan, the first singlet excited state (S_1) was obtained with TD-DFT using the last STS orbitals as an initial SCF guess. Starting from the same orbitals and STS geometries at each value of the reaction coordinate, we performed optimization of S_0, thus obtaining the ground state energy profile in the spin-unrestricted DFT approach.

4. RESULTS AND DISCUSSION

4.1. Linear Spectral Properties of 1. Photoisomerization proceeded for diarylethene **1** are shown in Figure 3. A solution of the OF is colorless (no absorption bands in the visible spectral range) and becomes colored during the cyclization reaction OF → CF induced by UV irradiation. The reverse process CF → OF also was observed under irradiation in the visible region. The steady-state absorption spectra of the individual OF and CF of **1** and their kinetic transformations OF → CF in hexane and DCM are presented in Figure 4. The values of the direct, Φ_{OC}, and reverse, Φ_{CO}, photochromic quantum yields of **1** are indicated in Table 1 along with other major photophysical parameters. According to this data, photochrome **1** exhibited extremely high

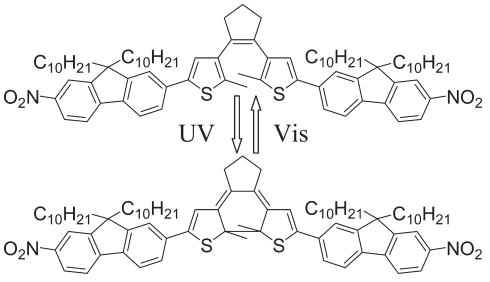

Figure 3. Molecular structures of the OF and CF isomers of photochrome **1**.

values of $\Phi_{OC} \approx 0.9-1.0$ in nonpolar solvents (hexane, cyclohexane), whereas the efficiency of the reverse reaction was lower than the ring closure by up to 3−3.5 orders of magnitude. Thus, the conversion efficiency of the direct photochromic transformation (OF → CF) exceeds 99% upon irradiation at λ_{abs}^{max} of the OF in nonpolar solvents, which is indicative of the large amount of photochemically convertible isomers of **1** in these media. No essential dependence of Φ_{OC} and Φ_{CO} on solvent viscosity was observed in nonpolar solvents. In polar DCM the efficiency of direct photochromic transformation of **1** decreased significantly ($\Phi_{OC} \approx 4 \times 10^{-2}$) in contrast to the reverse quantum yield Φ_{CO}, which decreased by 2−3 fold relative to in nonpolar solvents. As in nonpolar hexane, nearly full (~98%) direct photochromic transformation of **1** (OF → CF) was observed in polar DCM. This means that the amount of convertible isomers in solution is large and independent of solvent polarity.

The maximum extinction coefficients of **1** were relatively high ($\sim(5-6) \times 10^4$ M^{-1} cm^{-1}) and decreased by 25−30% under cyclization, which is a typical trend for diarylethene photochromes.[38,52] The reliable analysis of the steady-state fluorescence and excitation spectra of **1** (Figure 5) was performed only in more polar DCM, where the value of $\Phi_{OC} \ll 1.0$ and fluorescence quantum yields of the OF, Φ_{OF}^{FL}, and CF, Φ_{CF}^{FL}, were not extremely low (see Table 1). As follows from Figure 5a, the excitation spectrum of the OF in DCM (curve 3) nicely overlapped with the corresponding absorption contour (curve 1). At first thought,

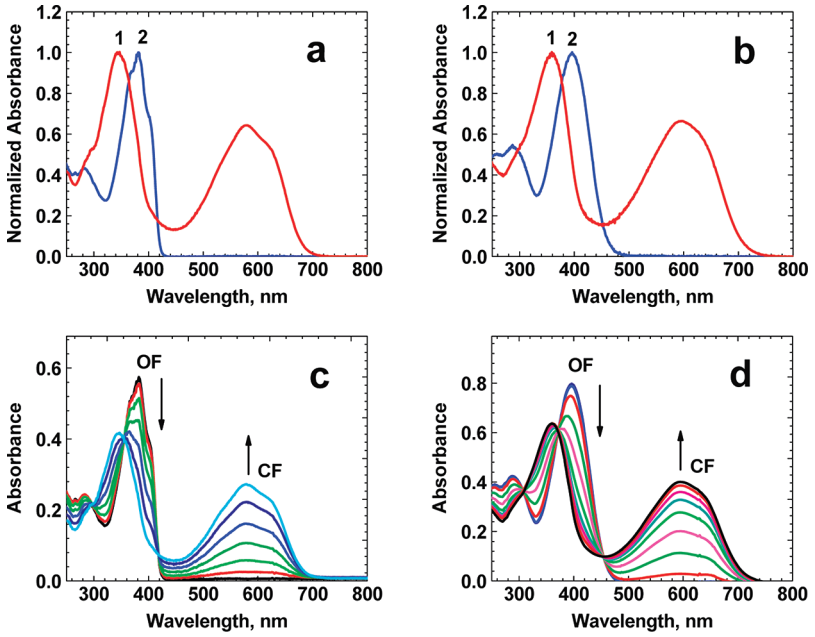

Figure 4. (a, b) Normalized steady-state absorption spectra of the OF (2) and CF (1) of **1** and (c, d) kinetic changes OF → CF under cw laser irradiation at 405 nm in (a, c) hexane and (b, d) DCM, respectively.

Table 1. Major Photophysical Parameters of 1 in Organic Solvents with Different Polarity, Δf^*, and Viscosity η^a

	hexane	cyclohexane	DCM
Δf^*	8×10^{-5}	2.5×10^{-4}	0.217
η, cP	0.313	0.97	0.4
λ_{abs}^{max}, nm (OF)	381 ± 1	385 ± 1	396 ± 1
λ_{abs}^{max}, nm (CF)	345 ± 1	347 ± 1	359 ± 1
$\varepsilon^{max} \times 10^{-3}$, M^{-1} cm^{-1} (OF)	54 ± 5	62 ± 5	52 ± 5
$\varepsilon^{max} \times 10^{-3}$, M^{-1} cm^{-1} (CF)	39 ± 4	46 ± 4	42 ± 4
Φ_{OC} (λ_{exc} = 405 nm)	1.0 ± 0.2	0.9 ± 0.2	0.04 ± 0.004
Φ_{CO} (λ_{exc} = 532 nm)	(8.3 ± 1) × 10^{-4}	(4.8 ± 0.6) × 10^{-4}	(2.3 ± 0.3) × 10^{-4}
Φ_{OF}^{FL}	(3.3 ± 2) × 10^{-4}	<10^{-4}	(1.2 ± 0.4) × 10^{-2}
Φ_{CF}^{FL}	(3 ± 2) × 10^{-4}	(2 ± 1) × 10^{-3}	(5 ± 2) × 10^{-3}

[a] Absorption maxima, λ_{abs}^{max}; maximum extinction coefficients, ε^{max}; quantum yields of the photochromic transformations, Φ_{OC}, Φ_{CO} at corresponding excitation wavelengths, λ_{exc}, and fluorescence quantum yields, Φ_{OF}^{FL}, Φ_{CF}^{FL}, of the OF and CF, respectively. * Orientation polarizability $\Delta f = (\varepsilon - 1)/(2\varepsilon + 1) - (n^2 - 1)/(2n^2 + 1)$ (ε and n are the dielectric constant and refraction index of the medium, respectively).[37]

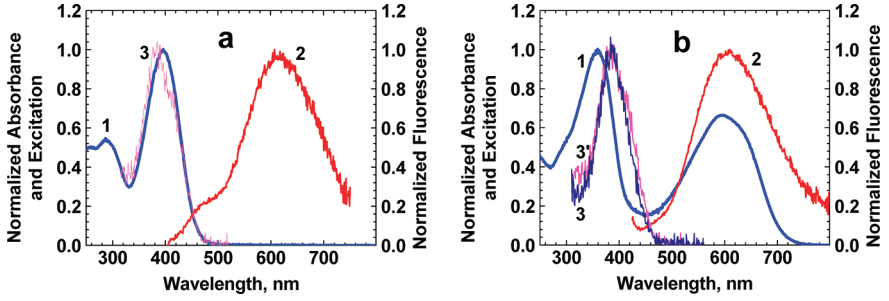

Figure 5. Steady-state absorption (1), fluorescence (2), and excitation (3, 3′) spectra of the (a) OF and (b) CF of **1** in DCM. Curve 3′ in b is identical to curve 3 in a and presented for comparison with curve 3 in b. The observed wavelength for all excitation spectra was ~620 nm.

the fluorescence spectrum with maximum at ~620 nm (curve 2) should be a weak emission of the OF in DCM. On the other hand, nearly identical excitation and emission spectra (Figure 5b, curves 2, 3) were observed from the same solution after its full photochromic transformation OF → CF (>98%). This suggests that a small amount (1−2%) of highly fluorescent unconverted isomers

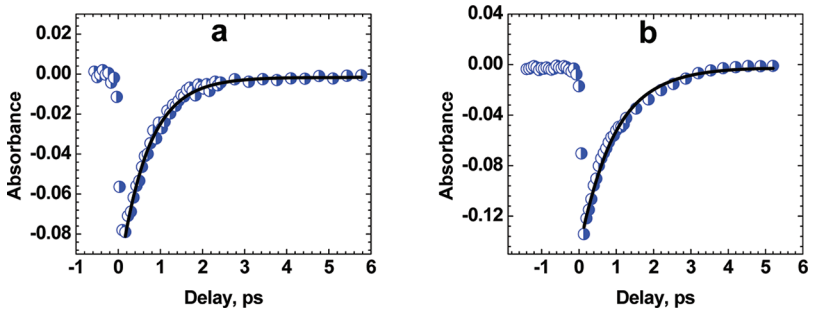

Figure 6. Transient absorbance profiles of **1** in DCM. (a) OF pumped at 405 nm and monitored at 425 nm. (b) CF pumped and monitored at 600 nm. Solid curves are the single exponential fits (see text).

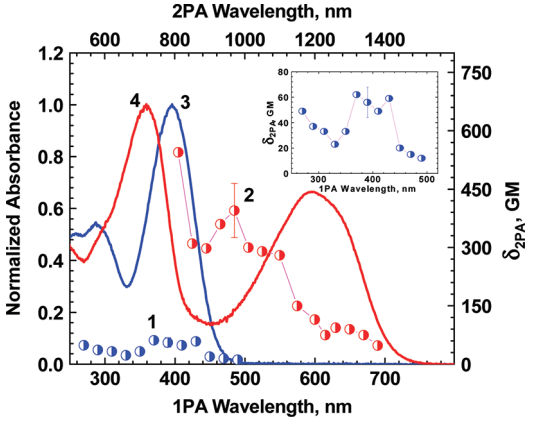

Figure 7. 2PA spectra of the OF (1) and CF (2) with corresponding linear one-photon absorption spectra of the OF (3) and CF (4) of **1** in DCM. The inset is a scaled 2PA contour of the OF (curve 1).

of **1** exist in solution. These isomers were likely responsible for the weak emission properties of **1** but did not effect photochromic reaction of the convertible isomers.

4.2. Transient Absorption Kinetics. Transient absorption measurements were performed in order to estimate the corresponding rate constants of the cyclization and cycloreversion reactions of **1** and better understand the fast photoisomerization that was observed. The time profiles of transient absorbance of the OF and CF of **1** in DCM, obtained by a femtosecond pump−probe technique, are presented in Figure 6. Corresponding solutions with pure OF and CF were prepared before pump−probe measurements. The negative absorption signals observed at 425 (Figure 6a) and 600 nm (Figure 6b) exhibited nearly monoexponential decay and can be ascribed to the depopulation of the OF and CF ground states, respectively. In the case of sufficiently low photochromic quantum yields ($\{\Phi_{OC}, \Phi_{CO}\} \ll 1.0$) the time constants of the recovering processes for OF, $\tau_{OF} \approx (0.7 \pm 0.1)$ ps, and CF, $\tau_{CF} \approx (0.9 \pm 0.1)$ ps, should be consistent with corresponding lifetimes of the first excited state S_1 of OF and CF, respectively. It should be noted that no long components (~5−10 ps) in the negative absorbance decay which can be associated with vibrational thermalization effects in the ground state[32,34] were observed. The obtained lifetimes, τ_{OF} and τ_{CF}, along with the quantum yields Φ_{OC} and Φ_{CO}, allowed determination of the rate constants of the photochromic transformation, $k_{OF} = \Phi_{OF}/\tau_{OF} \approx 5.7 \times 10^{10}$ s^{-1} (OF → CF) and $k_{CF} = \Phi_{CF}/\tau_{CF} \approx 2.6 \times 10^{8}$ s^{-1} (CF → OF) for **1** in DCM. A comprehensive analysis of the data in Table 1 allows for the estimation of the corresponding rate constant for **1** in hexane as $k_{OF} > 1 \times 10^{12}$ s^{-1}. It should be mentioned that direct measurement of this value by transient absorption methodology under the employed technical parameters of the flow cell system were nearly impossible due to extremely high quantum yield of the photochromic transformation of **1** in hexane ($\Phi_{OC} \simeq 1.0$).

4.3. 2PA Spectra of 1. To assess the two-photon absorptivity and sensitivity of diarylethene **1**, we obtained the degenerate 2PA spectra of the OF and CF over a broad spectral range by an open aperture femtosecond Z-scan method[44] with data presented in Figure 7. The values of the OF 2PA cross sections were relatively low ($\delta_{2PA} \sim 50-70$ GM) with a well-defined maximum in the range $\delta_{2PA}/2 \approx 380-420$ nm (curve 1) that closely overlapped with the corresponding linear (one-photon allowed) absorption band at ≈400 nm (curve 3). The nature of this 2PA maximum, which is electronically forbidden in symmetric molecules can be explained by strong vibronic interactions playing an important role in their nonlinear optical properties.[45,53] It should be noted that the OF 2PA spectrum was similar to that of a separate fluorene compound with NO_2 substituents in 2 position[54] and related diarylethene derivatives.[55] This suggests that the OF of **1** possesses a restricted π-conjugation length, resulting in relatively small transition dipoles. A strong enhancement of 2PA efficiency (up to 1 order of magnitude) with $\delta_{2PA} \sim 450-600$ GM was observed after photocyclization of **1** in DCM (curve 2) to produce the CF. Apparently, this enhancement reflects a drastic increase in π-conjugation length upon cyclization. In contrast to the OF, the 2PA spectrum of the CF exhibited a long wavelength maximum at $\delta_{2PA}/2 \approx 500$ nm that did not overlap with the main one-photon allowed absorption band of CF. It is reasonable to assume that the photochromic transformation of **1** is independent of the type of excitation (one- or two-photon), and compound **1** can exhibit efficient reversible first-order photoswitching via 2PA in the spectral range 800−980 nm that is potentially useful in a number of related applications, including high-density 3D optical data storage[38] and molecular optical switching.[4]

4.4. Quantum Chemical Analysis. To gain insight into the efficient photoisomerization of diarylethene **1**, we performed a quantum chemical investigation. The resulting MEPs of **1** are illustrated in Figure 8. We can conclude that the ground state surface has a high (about 2 eV) barrier between the OF and CF basins, which provides good thermal stability of both isomers. The transition state on the S_0 surface was observed at about 2.1 Å of the cyclization bond length. The MEP for the S_1 state also has two minima at the regions corresponding to the OF and CF.

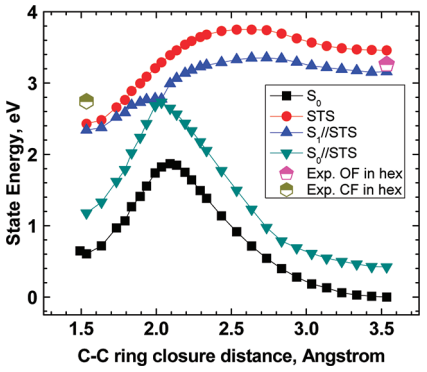

Figure 8. Ground- and excited-state energy profiles. The lowest curve corresponds to the relaxed scan along the ground electronic state. The upper curve is the relaxed scan, which was done using STS-M05-1.25X/6-31G*/PCM(n-hexane). The other two curves were obtained at the STS optimized geometries: TD//STS stands for the total TD-DFT energy of the lowest singlet state, and S_0//STS is the SCF energy M05-1.25X/6-31G*/PCM(n-hexane). Single dots correspond to the energy of experimental absorption maxima. The conical intersection of S_1/S_0 surfaces is located on the relaxed energy profile of the first excited state, which provides a very fast photocyclization.

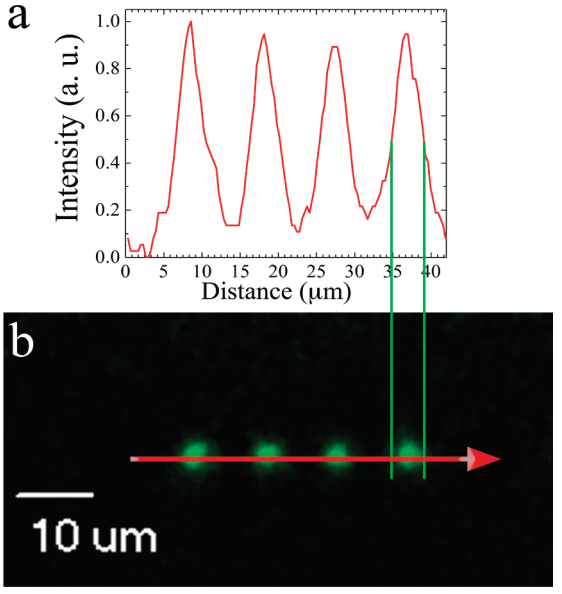

Figure 9. (a) Inverted signal intensity versus distance (μm) along (b) pixels traced by red arrow. Voxels recorded in photoreactive material consisting (b) of **1** and Rhodamine 6G in PMMA. Two-photon recording by inducing conversion OF to CF. Fluorescence of Rhodamine 6G was interrogated for two-photon fluorescence readout. After channel inversion, green pixels show the area within the material where fluorescence intensity was a minimum.

However, unlike the S_0 surface, it has a pericyclic minimum between them instead of a transition state. A specific feature of **1** is an immediate proximity of this minimum to a conical intersection of S_0 and S_1 states. This fact determines an ultrafast nonradiative decay $S_1 \rightarrow S_0$: center of a wave package on the S_1 surface stays close to the MEP and hence rapidly propagates to S_0 through the conical intersection. As one can see from Figure 8, the avoided crossing where S_0 and S_1 surfaces approach each other (with TD-DFT excitation energy of c.a. 0.008 eV) was found approximately at 2.0 Å step of the reaction coordinate. It is not exactly above the ground-state maximum, but rather shifted toward the CF basin. This finding can mean that if the system reaches the pericyclic minimum on the S_1 surface with small kinetic energy distributed along the reaction coordinate, it decays to the S_0 state and then relaxes to the CF rather than OF basin. Optimization of the ground state started from this point and converged to the CF structure, which confirmed our assumption.

The energy barrier along the S_1 MEP for evolution from the OF to the pericyclic minimum is about 0.2 eV. The barrier along S_1 from the CF to the pericyclic minimum is about 0.4 eV, and from the CF to OF is about 1.0 eV. The same barrier of 0.2 eV can be considered to separate OF and CF regions when propagating along the excited MEP from the side of the OF. A similar barrier from the CF to OF is much higher. It is about 1.0 eV and prevents cycloreversion along the excited state. The S_1 state in the CF region is lower in energy by 0.8 eV than that in the OF. They are separated by 1.0 eV barrier when going from the CF to OF regions and by 0.2 eV when going in the opposed direction. Thus, evolution along S_1 surface from the OF to CF is irreversible. The slope of the S_1 MEP from the OF side toward the conical intersection is steep, which means high kinetic energy assigned to the motion toward cyclization. This explains the high quantum yield of photocyclization.

One can expect that after absorption of photon, the system vertically excited to the S_1 and has enough energy to overcome the 0.2 eV barrier. During evolution energy dissipates through the solvent, and the system cannot return to the OF. From the other side (CF), after a vertical excitation the system can, probably, also overcome the barrier of 0.4 eV. This means that cycloreversion after photoabsorption by a CF isomer is also possible. However, the slope of the S_1 MEP from that side in the region of the conical intersection is flat, which means it might not have enough energy for cycloreversion even after passing through the S_1/S_0 intersection. This is a possible explanation of a relatively low yield of cycloreversion. As follows from this analysis, there are two factors defining the cyclization quantum yield: the barrier from the initial, Franck−Condon, region to the pericyclic minimum, and the slope of the MEP in the region of the conical intersection. The high photoswitching rate of the system is defined by close proximity of the S_1/S_0 intersection to the S_1 MEP.

4.5. Optical Data Recording. The potential utility of **1** in optical data storage was demonstrated in a system consisting of PMMA doped with **1** and Rhodamine 6G. In this system, voxels representing data were registered ("written") inducing the photoisomerization of **1** from the OF to the CF by 2PA at 750 nm). Once the film of the photoreactive media was placed on the microscope stage and immobilized, the stage was "parked" at a specific location and exposed for 2 ms. The voxels were "readout" by recording the fluorescence of Rhodamine 6G induced by 2PA (750 nm; 130 mW; 40x). This indirect readout methodology was employed to avoid direct interrogation of the CF of **1**, providing a relatively destructive readout. The fluorescence of Rhodamine 6G overlaps with absorption of the CF. Thus, the intensity of the Rhodamine 6G fluorescence is a measure of the relative amount of CF vs OF (hence data recording).[38,56] In the areas where the materials had been exposed little to no fluorescence was observed due to the reabsorption of the Rhodamine 6G fluorescence by the CF of compound **1** that had been previously generated in the writing process. Once the fluorescence had been recorded, the channels

were inverted resulting in fluorescent pixels showing minimum to no intensity and nonfluorescent pixels showing the highest intensities (Figure 9). A signal intensity versus distance plot (Figure 9a) was traced along the red line shown in the inverted fluorescence micrograph (Figure 9b) to illustrate how clearly the data can be read out, enabling a binary data optical data storage.

5. CONCLUSIONS

A new diarylethene-fluorenyl derivative (**1**) was synthesized and photophysically characterized by means of steady-state spectroscopy and nonlinear optical techniques. Cyclization and cycloreversion processes of **1** were investigated at room temperature in hexane, cyclohexane and DCM. A very high quantum yield of nearly 1.0 was observed for the direct photochromic transformation of **1** in nonpolar medium. Femtosecond transient absorption profiles of the OF and CF of **1** revealed a fast electronic relaxation of their first excited states S_1 with corresponding lifetimes ~0.7 and ~0.9 ps, respectively. The rate constants of the photochromic reactions of OF and CF of **1** were determined in DCM as $k_{OF} \approx 5.7 \times 10^{10}\ s^{-1}$ and $k_{CF} \approx 2.6 \times 10^{8}\ s^{-1}$, respectively. Based on these results and the corresponding values of Φ_{OC} that were obtained in DCM and hexane, we can estimate that the time for direct photochromic transformation of **1** in nonpolar medium should be less than 1 ps. The fast photochromic transformation of **1** and its high quantum yield was interpreted by analysis of minimum energy profiles. Quantum chemical investigation involving Slater transition state method followed by TD-DFT correction was used to approximate the excited state potential energy surface. Specific photochemical features were attributed to the large energy difference between OF and CF isomers in the excited state and to the close proximity of the conical intersection to the MEP. Degenerate 2PA spectra of **1** were obtained over a broad spectral range 560−980 nm (OF) and 810−1380 nm (CF) by an open aperture Z-scan method using 1 kHz femtosecond excitation. A significant increase in the 2PA cross section from $\delta_{2PA} \sim 50-70$ GM for the OF up to $\delta_{2PA} \sim 450-600$ GM for the CF was observed, ascribed to the pronounced extension of its π-conjugation length upon photocyclization. An example of a photochromic medium for two-photon optical recording based on PMMA doped films containing the new diarylethene-fluorene compound **1** was presented with preliminary two-photon data recording and readout, indicating that diarylethene **1** will be an interesting candidate for those interested in photochromic data storage and optical switching.

■ ACKNOWLEDGMENT

We acknowledge the National Science Foundation (ECCS-0925712, CHE-0840431, and CHE-0832622), U.S. Civilian Research and Development Foundation (UKB2-2923-KV-07), the Ministry of Education and Science of Ukraine (Grant M/49-2008), and the U.S. National Academy of Sciences (PSA-P210877) for support of this work.

■ REFERENCES

(1) Yassar, A.; Garnier, F.; Jaafari, H.; Rebiere-Galy, N.; Frigoli, M.; Moustrou, C.; Samat, A.; Guglielmetti, R. *Appl. Phys. Lett.* **2002**, *80*, 4297.
(2) Berkovic, G.; Krongauz, V.; Weiss, V. *Chem. Rev.* **2000**, *100*, 1741.
(3) Yun, C.; You, J.; Kim, J.; Huh, J.; Kim, E. *J. Photochem. Photobiol., C* **2009**, *10*, 111.
(4) Xu, L.; Zhao, Z. J.; Xing, Y. J.; Lu, P. *J. Zhejiang Univ., Sci., A* **2008**, *9*, 1590.
(5) van der Molen, S. J.; Liao, J. H.; Kudernac, T.; Agustsson, J. S.; Bernard, L.; Calame, M.; van Wees, B. J.; Feringa, B. L.; Schonenberger, C. *Nano Lett.* **2009**, *9*, 76.
(6) Paterson, J.; Natansohn, A.; Rochon, P.; Callender, C. L.; Robitaille, L. *Appl. Phys. Lett.* **1996**, *69*, 3318.
(7) Rochon, P.; Natansohn, A.; Callender, C. L.; Robitaille, L. *Appl. Phys. Lett.* **1997**, *71*, 1008.
(8) Kawata, S.; Kawata, Y. *Chem. Rev.* **2000**, *100*, 1777.
(9) Liang, Y. C.; Dvornikov, A. S.; Rentzepis, P. M. *Tetrahedron Lett.* **1999**, *40*, 8067.
(10) Toriumi, A.; Herrmann, J. M.; Kawata, S. *Opt. Lett.* **1997**, *22*, 555.
(11) Chen, B. Z.; Wang, M. Z.; Li, C.; Xia, H. M.; Tian, H. *Synth. Met.* **2003**, *135*, 491.
(12) Rumi, M.; Ehrlich, J. E.; Heikal, A. A.; Perry, J. W.; Barlow, S.; Hu, Z. Y.; McCord-Maughon, D.; Parker, T. C.; Rockel, H.; Thayumanavan, S.; Marder, S. R.; Beljonne, D.; Bredas, J. L. *J. Am. Chem. Soc.* **2000**, *122*, 9500.
(13) Lu, Y. M.; Hasegawa, F.; Ohkuma, S.; Goto, T.; Fukuhara, S.; Kawazu, Y.; Totani, K.; Yamashita, T.; Watanabe, T. *J. Mater. Chem.* **2004**, *14*, 1391.
(14) Diaspro, A.; Federici, F.; Viappiani, C.; Krol, S.; Pisciotta, M.; Chirico, G.; Cannone, F.; Gliozzi, A. *J. Phys. Chem. B* **2003**, *107*, 11008.
(15) Ogawa, K.; Kobuke, Y. *Org. Biomol. Chem.* **2009**, *7*, 2241.
(16) Belfield, K. D.; Liu, Y.; Negres, R. A.; Fan, M.; Pan, G.; Hagan, D. J.; Hernandez, F. E. *Chem. Mater.* **2002**, *14*, 3663.
(17) Wei, F.; Kun, H.; Mei-Xiang, W. *Chin. Phys.* **2005**, *14*, 306.
(18) Liang, Y. C.; Dvornikov, A. S.; Rentzepis, P. M. *Macromolecules* **2002**, *35*, 9377.
(19) Irie, M.; Mohri, M. *J. Org. Chem.* **1988**, *53*, 803.
(20) Irie, M. *Chem. Rev.* **2000**, *100*, 1683.
(21) Gilat, S. L.; Kawai, S. H.; Lehn, J. M. *J. Chem. Soc., Chem. Commun.* **1993**, 1439.
(22) Tsivgoulis, G. M.; Lehn, J. M. *Angew. Chem., Int. Ed.* **1995**, *34*, 1119.
(23) Cho, H. G.; Cheong, B. S. *Bull. Korean Chem. Soc.* **1998**, *19*, 308.
(24) Higashiguchi, K.; Matsuda, K.; Kobatake, S.; Yamada, T.; Kawai, T.; Irie, M. *Bull. Chem. Soc. Jpn.* **2000**, *73*, 2389.
(25) Miyasaka, H.; Araki, S.; Tabata, A.; Nobuto, T.; Mataga, N.; Irie, M. *Chem. Phys. Lett.* **1994**, *230*, 249.
(26) Kim, E.; Park, J.; Cho, S. Y.; Kim, N.; Kim, J. H. *ETRI J.* **2003**, *25*, 253.
(27) Saita, S.; Yamaguchi, T.; Kawai, T.; Irie, M. *ChemPhysChem* **2005**, *6*, 2300.
(28) Shim, S.; Eom, I.; Joo, T.; Kim, E.; Kim, K. S. *J. Phys. Chem. A* **2007**, *111*, 8910.
(29) Clark, A. E. *J. Phys. Chem. A* **2006**, *110*, 3790.
(30) Chen, D. Z.; Wang, Z.; Zhang, H. H. *J. Mol. Struct. Theochem* **2008**, *859*, 11.
(31) Laurent, A. D.; Andre, J. M.; Perpete, E. A.; Jacquemin, D. *J. Photochem. Photobiol., A* **2007**, *192*, 211.
(32) Ishibashi, Y.; Murakami, M.; Miyasaka, H.; Kobatake, S.; Irie, M.; Yokoyama, Y. *J. Phys. Chem. C* **2007**, *111*, 2730.
(33) Ishibashi, Y.; Katayama, T.; Ota, C.; Kobatake, S.; Irie, M.; Yokoyama, Y.; Miyasaka, H. *New J. Chem.* **2009**, *33*, 1409.
(34) Ishibashi, Y.; Okuno, K.; Ota, C.; Umesato, T.; Katayama, T.; Murakami, M.; Kobatake, S.; Irie, M.; Miyasaka, H. *Photochem. Photobiol. Sci.* **2010**, *9*, 172.
(35) Lucas, L. N.; de Jong, J. J. D.; van Esch, J. H.; Kellogg, R. M.; Feringa, B. L. *Eur. J. Org. Chem.* **2003**, 155.
(36) Belfield, K. D.; Schafer, K. J.; Mourad, W.; Reinhardt, B. A. *J. Org. Chem.* **2000**, *65*, 4475.
(37) Lakowicz, J. R. *Principles of Fluorescence Spectroscopy*; Kluwer: New York, 1999.

(38) Corredor, C. C.; Huang, Z. L.; Belfield, K. D.; Morales, A. R.; Bondar, M. V. *Chem. Mater.* **2007**, *19*, 5165.
(39) Lepkowicz, R. S.; Przhonska, O. V.; Hales, J. M.; Hagan, D. J.; Van Stryland, E. W.; Bondar, M. V.; Slominsky, Y. L.; Kachkovski, A. D. *Chem. Phys.* **2003**, *286*, 277.
(40) Miyasaka, H.; Murakami, M.; Okada, T.; Nagata, Y.; Itaya, A.; Kobatake, S.; Irie, M. *Chem. Phys. Lett.* **2003**, *371*, 40.
(41) Palfrey, S. L.; Heinz, T. F. *J. Opt. Soc. Am. B* **1985**, *2*, 674.
(42) Bradley, C. W. W.; Taylor, R. A.; Ryan, J. F.; Mitchell, E. W. J. *J. Phys. Cond. Mat.* **1989**, *1*, 2715.
(43) Idrissi, A.; Ricci, M.; Bartolini, P.; Righini, R. *J. Chem. Phys.* **1999**, *111*, 4148.
(44) Sheik-Bahae, M.; Said, A. A.; Wei, T. H.; Hagan, D. J.; Van Stryland, E. W. *IEEE J. Quant. Electron.* **1990**, *26*, 760.
(45) Belfield, K. D.; Bondar, M. V.; Hernandezt, F. E.; Przhonska, O. V.; Yao, S. *J. Phys. Chem. B* **2007**, *111*, 12723.
(46) Bearpark, M. J.; Ogliaro, F.; Vreven, T.; Boggio-Pasqua, M.; Frisch, M. J.; Larkin, S. M.; Morrison, M.; Robb, M. A. *J. Photochem. Photobiol., A* **2007**, *190*, 207.
(47) Nakamura, S.; Yokojima, S.; Uchida, K.; Tsujioka, T.; Goldberg, A.; Murakami, A.; Shinoda, K.; Mikami, M.; Kobayashi, T.; Kobatake, S.; Matsuda, K.; Irie, M. *J. Photochem. Photobiol., A* **2008**, *200*, 10.
(48) Mikhailov, I. A.; Belfield, K. D.; Masunov, A. E. *J. Phys. Chem. A* **2009**, *113*, 7080.
(49) Patel, P. D.; Masunov, A. E. *J. Phys. Chem. A* **2009**, *113*, 8409.
(50) Mikhailov, I. A.; Bondar, M. V.; Belfield, K. D.; Masunov, A. E. *J. Phys. Chem. C* **2009**, *113*, 20719.
(51) Frisch, M. J.; Trucks, G. W.; Schlegel, H. B.; Scuseria, G. E.; Robb, M. A.; Cheeseman, J. R.; Scalmani, G.; Barone, V.; Mennucci, B.; Petersson, G. A.; Nakatsuji, H.; Caricato, M.; Li, X. H., H. P.; Izmaylov, A. F.; Bloino, J.; Zheng, G.; Sonnenberg, J. L.; Hada, M.; Ehara, M.; Toyota, K.; Fukuda, R.; Hasegawa, J.; Ishida, M.; Nakajima, T.; Honda, Y.; Kitao, O.; Nakai, H.; Vreven, T.; Montgomery, J., J. A.; Peralta, J. E.; Ogliaro, F.; Bearpark, M.; Heyd, J. J.; Brothers, E.; Kudin, K. N.; Staroverov, V. N.; Kobayashi, R.; Normand, J.; Raghavachari, K.; Rendell, A.; Burant, J. C.; Iyengar, S. S.; Tomasi, J.; Cossi, M.; Rega, N.; Millam, N. J.; Klene, M.; Knox, J. E.; Cross, J. B.; Bakken, V.; Adamo, C.; Jaramillo, J.; Gomperts, R.; Stratmann, R. E.; Yazyev, O.; Austin, A. J.; Cammi, R.; Pomelli, C.; Ochterski, J. W.; Martin, R. L.; Morokuma, K.; Zakrzewski, V. G.; Voth, G. A.; Salvador, P.; Dannenberg, J. J.; Dapprich, S.; Daniels, A. D.; Farkas, Ö.; Foresman, J. B.; Ortiz, J. V.; Cioslowski, J.; Fox, D. J. *Gaussian 09; Revision A.2 ed.*; Gaussian, Inc.: Wallingford CT, 2009.
(52) Santos, A. R.; Ballardini, R.; Belser, P.; Gandolfi, M. T.; Iyer, V. M.; Moggi, L. *Photochem. Photobiol. Sci.* **2009**, *8*, 1734.
(53) Terenziani, F.; Painelli, A.; Katan, C.; Charlot, M.; Blanchard-Desce, M. *J. Am. Chem. Soc.* **2006**, *128*, 15742.
(54) Belfield, K. D.; Bondar, M. V.; Hernandez, F. E.; Masunov, A. E.; Mikhailov, I. A.; Morales, A. R.; Przhonska, O. V.; Yao, S. *J. Phys. Chem. C* **2009**, *113*, 4706.
(55) Corredor, C. C.; Belfield, K. D.; Bondar, M. V.; Przhonska, O. V.; Hernandez, F. E.; Kachkovsky, O. D. *J. Photochem. Photobiol., A* **2006**, *184*, 177.
(56) Corredor, C. C.; Huang, Z.-L.; Belfield, K. D. *Adv. Mater.* **2006**, *18*, 2910–2914.